



Deposited via The University of Leeds.

White Rose Research Online URL for this paper:

<https://eprints.whiterose.ac.uk/id/eprint/168059/>

Version: Accepted Version

Article:

Alosaimi, M, Lesnic, D and Nho Hào, D (2021) Identification of the forcing term in hyperbolic equations. *International Journal of Computer Mathematics*, 98 (9). pp. 1877-1891. ISSN: 0020-7160

<https://doi.org/10.1080/00207160.2020.1854744>

© 2020 Informa UK Limited, trading as Taylor & Francis Group. This is an author produced version of an article published in *International Journal of Computer Mathematics*.
Uploaded in accordance with the publisher's self-archiving policy.

Reuse

Items deposited in White Rose Research Online are protected by copyright, with all rights reserved unless indicated otherwise. They may be downloaded and/or printed for private study, or other acts as permitted by national copyright laws. The publisher or other rights holders may allow further reproduction and re-use of the full text version. This is indicated by the licence information on the White Rose Research Online record for the item.

Takedown

If you consider content in White Rose Research Online to be in breach of UK law, please notify us by emailing eprints@whiterose.ac.uk including the URL of the record and the reason for the withdrawal request.

Identification of the forcing term in hyperbolic equations

M. Alosaimi^{1,2}, D. Lesnic¹ and Dinh Nho Hào³

¹Department of Applied Mathematics, University of Leeds, Leeds LS2 9JT, UK

²Department of Mathematics, Taif University, Taif P.O. Box 888, Saudi Arabia

³Hanoi Institute of Mathematics, 18 Hoang Quoc Viet Road, Hanoi, Vietnam

E-mails: mmaal@leeds.ac.uk (M. Alosaimi), amt5ld@maths.leeds.ac.uk (D. Lesnic), hao@math.ac.vn (D.N. Hào)

Abstract

We investigate the problem of recovering the possibly both space and time-dependent forcing term along with the temperature in hyperbolic systems from many integral observations. In practice, these average weighted integral observations can be considered as generalized interior point measurements. This linear but ill-posed problem is solved using the Tikhonov regularization method in order to obtain the closest stable solution to a given *a priori* known initial estimate. We prove the Fréchet differentiability of the Tikhonov regularization functional and derive a formula for its gradient. This minimization problem is solved iteratively using the conjugate gradient method. The numerical discretization of the well-posed problems, that are: the direct, adjoint and sensitivity problems that need to be solved at each iteration is performed using finite difference methods. Numerical results are presented and discussed for one and two-dimensional problems.

Keywords: Inverse force problem; hyperbolic equations; integral observations; Tikhonov's regularization; conjugate gradient method.

1 Introduction

Hyperbolic PDE's and, in particular, the wave equation, govern many wave propagation phenomena, e.g. in acoustic scattering, vibrations of a string, etc. When it comes to inverse modelling probably the most investigated are obstacle identification problems in acoustic scattering, see Colton and Kress (2013), followed by the reconstruction of the speed of wave propagation, see Isakov (1998, Section 8.1). On the other hand, many engineering applications related to unknown force loads and control of seismic, wind or noise exatations, modelled as inverse force problems for hyperbolic PDE's have been less investigated possibly due to their high non-uniqueness of solution that occurs in general.

Practical examples of inverse force problems include: (i) the reconstruction of time-dependent external forces in a vibrating system from the measurements of the displacement and velocity at different times, see Huang (2001); (ii) seismic events such as implosion, explosion or earthquake, which can be modelled as a point moment tensor forcing in the elastic wave equation, and can then be estimated using measurements of waveforms, see Sjögreen and Petersson (2014); (iii) ocean acoustics, where point forces in the ocean are to be determined from measurements of the acoustic pressure at an array of hydrophones, see Collins and Kuperman (1994).

Prior to this study, the inverse force problem of determining the free term in the right-hand side of hyperbolic PDE's has been investigated in some works, see e.g. Cannon and Dunninger (1970), Amirov (1987), Yamamoto (1995), Hasanov (2009), Hussein and Lesnic (2014), Vabishchevich (2019). For more detail, see also the PhD thesis of Hussein (2016) and the references therein. However, in all these works, the force function was sought as a function depending solely on either time or space. This restriction is needed because otherwise the inverse problem does not have a unique solution, unless the main dependent variable $u(x, t)$ is available/measured at all points (x, t) in the space-time solution domain, or a certain conductivity parameter is varied, see Abasheeva (2009). However, as proposed in this study, given some known *a priori* estimate $f^*(x, t)$ of the real practical solution, we can determine the (unique) closest force $f(x, t)$ to $f^*(x, t)$ which together with $u(x, t)$ satisfy in the weak sense the initial-boundary value problem for hyperbolic PDE's and match a finite set of integral observations. This formulation is described in the next section.

2 The mathematical formulation

Let $\Omega \subset \mathbb{R}^d$, $d = 1, 2, 3$, be an open bounded domain with a sufficiently smooth boundary $\partial\Omega$. Denote the cylinder $Q_T := \Omega \times (0, T]$, where $T > 0$, and the lateral surface $S_T := \partial\Omega \times (0, T]$. We consider the following general second-order linear hyperbolic PDE

$$u_{tt} - \nabla \cdot (A \nabla u) + b(x, t)u = F(x, t), \quad (x, t) \in Q_T, \quad (2.1)$$

where $b \geq 0$ is a given material property coefficient, $A = (a_{ij}(x, t))_{i,j=1,\dots,d}$ is the conductivity tensor which is assumed symmetric and positive definite, $u(x, t)$ represents the displacement, and $F(x, t)$ is a force acting on the system. In the inverse problem, these two latter quantities $u(x, t)$ and $F(x, t)$ are unknown. Equation (2.1) is quite general and models a wide range of wave-type phenomena including the thermal wave model of bio-heat transfer, see Özen et al. (2008), obtained by replacing in (2.1) the term u_{tt} by $\varepsilon u_{tt} + u_t$ with $\varepsilon > 0$ being small, or the wave equation obtained by replacing in (2.1) the term u_{tt} by $c^{-2}(x)u_{tt}$ with $c(x) > 0$ representing the wave speed.

Associated with (2.1), we have prescribed the initial conditions

$$u|_{t=0} = u_0(x), \quad u_t|_{t=0} = v_0(x), \quad x \in \Omega, \quad (2.2)$$

and either the Robin boundary condition

$$\frac{\partial u}{\partial \mathcal{N}} + \sigma u = \varphi \quad \text{on } S_T, \quad (2.3)$$

or, the Dirichlet boundary condition

$$u = \psi \quad \text{on } S_T. \quad (2.4)$$

In (2.2), u_0 and v_0 represent the initial displacement and velocity, respectively, and φ and ψ are given functions in $L^2(S_T)$. In (2.3), $L^\infty(S_T) \ni \sigma \geq 0$ is a given transfer coefficient and the normal derivative is defined so as to take into account the anisotropy of the conductivity $A = (a_{ij})_{i,j=\overline{1,d}}$, namely,

$$\frac{\partial u}{\partial \mathcal{N}} := \sum_{i,j=1}^d (a_{ij}(x, t) u_{x_j}) \cos(\nu, x_i) \quad \text{on } S_T, \quad (2.5)$$

where ν is the outward unit normal to the boundary $\partial\Omega$ and $\cos(\nu, x_i)$ is the direction cosine with the x_i -axis for $i = \overline{1,d}$. Remark that the Robin boundary condition (2.3) incorporates the Neumann boundary condition (obtained by taking $\sigma = 0$) and the homogeneous Dirichlet boundary condition (obtained by taking $\sigma = \infty$) given by

$$u = 0 \quad \text{on } S_T. \quad (2.6)$$

The latter condition (2.6) is also obtained when taking $\psi = 0$ in (2.4). In the above model (2.1)-(2.3) or (2.1), (2.2) and (2.4), if the coefficients b , a_{ij} and σ , and the functions F , u_0 , v_0 , φ or ψ are all known, then this gives rise to a direct problem whose well-posedness holds in various spaces. For example, the direct problem given by the hyperbolic equation (2.1) with

$$a_{ij} = a_{ji} \in C^1(\overline{Q_T}), \quad i, j = \overline{1,d}, \quad b \in C^1(\overline{Q_T}), \quad (2.7)$$

$$\lambda \|\xi\|_{\mathbb{R}^d}^2 \leq \sum_{i,j=1}^d a_{ij}(x, t) \xi_i \xi_j \leq \Lambda \|\xi\|_{\mathbb{R}^d}^2, \quad \forall \xi \in \mathbb{R}^d, \quad (2.8)$$

$$0 \leq b(x, t) \leq \mu_1, \quad \text{a.e. in } Q_T, \quad (2.9)$$

$$\text{for some positive constants } \lambda \text{ and } \Lambda \text{ and } \mu_1 \geq 0, \quad (2.10)$$

$$F \in L^2(Q_T), \quad (2.11)$$

satisfying the initial conditions (2.2) almost everywhere with

$$u_0 \in H_0^1(\Omega), \quad v_0 \in L^2(\Omega), \quad (2.12)$$

and the homogeneous Dirichlet boundary condition (2.6) has a unique weak solution in the space

$$W(0, T) := \{u \in C(0, T; H_0^1(\Omega)) \text{ with } u_t \in C(0, T; L^2(\Omega))\};$$

in fact, one has $u_{tt} \in L^2(0, T; H^{-1}(\Omega))$ and the stability estimate

$$\begin{aligned} \max_{t \in [0, T]} \left(\|u(\cdot, t)\|_{H_0^1(\Omega)} + \|u_t(\cdot, t)\|_{L^2(\Omega)} \right) + \|u_{tt}\|_{L^2(0, T; H^{-1}(\Omega))} \\ \leq C \left(\|F\|_{L^2(Q_T)} + \|u_0\|_{H_0^1(\Omega)} + \|v_0\|_{L^2(\Omega)} \right), \end{aligned} \quad (2.13)$$

for some positive constant C , holds, see Evans (1998, Section 7.2). The above solution satisfies equation (2.1) in the weak sense, i.e.

$$\begin{aligned} \int_0^T (u_{tt}, \eta)_{(H^{-1}(\Omega), H_0^1(\Omega))} dt + \int_{Q_T} ((A(x, t)\nabla u) \cdot \nabla \eta + b(x, t)u\eta) dx dt \\ = \int_{Q_T} F(x, t)\eta dx dt, \quad \forall \eta \in L^2(0, T; H_0^1(\Omega)). \end{aligned} \quad (2.14)$$

In this definition of a weak solution we have taken the test function η depending on both x and t , see Ladyzhenskaya (1985, p.157); however, it can also be taken to depend only on x , see Evans (1998, p.402). The boundary condition (2.6) is also satisfied since $u(\cdot, t) \in H_0^1(\Omega)$, $\forall t \in [0, T]$.

In the inverse problem the function $F(x, t)$ (together with $u(x, t)$) is unknown and has to be determined subject to additional information. Depending on the particular form of the function $F(x, t)$ that is *a priori* assumed and the type of additional information/measurement, we can have different inverse problem formulations, as follows:

- Inverse Problem (IP1):

$$F(x, t) = f(x)h(x, t) + g(x, t), \quad (2.15)$$

with $h(x, t)$ and $g(x)$ given. Find $f(x)$, given:

- $u(x, T)$ or $\int_0^T u(x, t)dt$ for $x \in \Omega$, see Cannon and Dunninger (1970), Prilepko et al. (2000, Section 8.2), Kozhanov and Safiullova (2010), Lesnic et al. (2016);
or
- $\frac{\partial u}{\partial N}$ on S_T , see Klibanov (1992), Engl et al. (1994), Yamamoto (1995), Hussein and Lesnic (2016a).

- Inverse Problem (IP2):

$$F(x, t) = f(t)h(x, t) + g(x, t), \quad (2.16)$$

with $h(x, t)$ and $g(x, t)$ given. Find $f(t)$, given:

- $\int_{\Omega} \omega(x)u(x, t)dx$ for $t \in [0, T]$, with $\omega(x)$ given, see Prilepko et al. (2000, Section 9.2), Hussein and Lesnic (2016b), Vabishchevich (2019);
or
- $\frac{\partial u}{\partial N}$ on S_T , see Rashedi and Sini (2015).

- Inverse Problem (IP3):

Find point forces from additional information, see El Badia and Ha-Duong (2001).

We remark that in some of these formulations accurate measurements should be available at all points $x \in \Omega$, which might be too intrusive from the practical point of view. In order to overcome this possible deficiency, we assume that we measure instead the average integrals

$$\ell_k u := \int_{\Omega} \omega_k(x)u(x, t)dx = h_k(t) \in L^2(0, T), \quad k = \overline{1, N}, \quad (2.17)$$

where N represents the number of measurements and $\omega_k \in L^\infty(\Omega)$ with $\int_\Omega \omega_k(x) dx > 0$ for $k = \overline{1, N}$ are given linearly independent weight functions. Then, with the multiple measurements (2.17) it might be possible to recover uniquely a sum of time-dependent forces $(f_k(t))_{k=\overline{1, N}}$ of the form

$$F(x, t) = g(x, t) + \sum_{k=1}^N f_k(t) h_k(x, t), \quad (2.18)$$

with $g(x, t)$ and $(h_k(t))_{k=\overline{1, N}}$ given, see Vabishchevich (2019).

Remark that the pointwise measurement of $u(x, t)$ at a discrete set of distinct points $\xi^1, \dots, \xi^N \in \Omega$ can be approximated by (2.17) if we take

$$\omega_k(x) = \frac{1}{|\Omega_k|} \chi_{\Omega_k}(x), \quad k = \overline{1, N}, \quad (2.19)$$

where Ω_k is a small neighbourhood of the point ξ^k such that $\Omega_k \cap \Omega_j = \emptyset, \forall j \neq k$, χ_{Ω_k} is the characteristic function of the domain Ω_k and $|\Omega_k|$ denotes its volume. Then, with the weights (2.19), the integrals (2.17) become

$$h_k(t) = \frac{1}{|\Omega_k|} \int_{\Omega_k} u(x, t) dx, \quad t \in (0, T), \quad k = \overline{1, N}, \quad (2.20)$$

and represent an average measurement around the point ξ^k which can be obtained by letting the neighbourhood Ω_k becoming vanishingly small.

Of course, in order to capture as much information as possible one should take N large, and in this case (2.20) has the set ξ^k for $k = 1, 2, \dots$ dense in Ω . But even so, under no further restriction on the general form of $F(x, t)$, there is still no unique solution globally. However, we can seek a quasi-solution (which is unique) by being the closest to an *a priori* estimate of the desired physical solution. Thus, assuming the form

$$F(x, t) = f(x, t) h(x, t) + g(x, t), \quad (2.21)$$

with $h \in L^\infty(Q_T)$ and $g \in L^2(Q_T)$ given, we minimize the Tikhonov regularization functional $J_\lambda : L^2(Q_T) \rightarrow \mathbb{R}_+$ defined by

$$J_\lambda(f) := \frac{1}{2} \sum_{k=1}^N \|\ell_k u - h_k\|_{L^2(0, T)}^2 + \frac{\lambda}{2} \|f - f^*\|_{L^2(Q_T)}^2, \quad (2.22)$$

where $\lambda > 0$ is a regularization parameter to be prescribed, $f^* \in L^2(Q_T)$ is a known *a priori* estimate of $f(x, t)$ and $u(x, t)$ satisfies the PDE

$$u_{tt} - \nabla \cdot (A \nabla u) + b(x, t) u = f(x, t) h(x, t) + g(x, t), \quad (x, t) \in Q_T, \quad (2.23)$$

and the initial and boundary conditions (2.2) and (2.3). Remark that this formulation has recently been adopted by Hào et al. (2017) for solving the corresponding inverse source problem for parabolic PDE's.

The plan of the remainder of the paper is as follows. In Section 3, we prove the Fréchet differentiability of the functional (2.22) and derive a formula for its gradient. Then, the CGM is described for the minimization procedure. Section 4 presents and discusses numerical results for typical benchmark examples in one and two dimensions and, finally, Section 5 highlights the conclusions of the paper.

3 The CGM

Consider, for simplicity, the homogeneous Dirichlet boundary condition (2.6) and analyse the inverse problem given by (2.23), (2.2), (2.6) and (2.17). The case of the Robin boundary condition (2.3) is similar.

First, it is easy to observe that if $\lambda > 0$, then there exists a unique solution to the minimization of (2.22). The sensitivity problem, adjoint problem and the gradient of the objective functional (2.22), whose solutions are required in the CGM, are derived in Sections 3.1-3.3, respectively.

3.1 The sensitivity problem

The sensitivity problem is found by first assuming that when the force function $f(x, t)$ undergoes a small variation $\Delta f(x, t)$, the temperature $u(x, t)$ is changed by a small amount $\Delta u(x, t)$. Then, substituting these perturbed quantities into the direct problem given by (2.23), (2.2) and (2.6) and subtracting the original direct problem from the resulting problem, we obtain the sensitivity problem given by

$$(\Delta u)_{tt} - \nabla \cdot (A \nabla (\Delta u)) + b(x, t) \Delta u = \Delta f(x, t) h(x, t), \quad (x, t) \in Q_T, \quad (3.1)$$

$$\Delta u(x, 0) = (\Delta u)_t(x, 0) = 0, \quad x \in \Omega, \quad (3.2)$$

$$\Delta u(x, t) = 0, \quad (x, t) \in S_T. \quad (3.3)$$

3.2 The adjoint problem

The adjoint problem is obtained via the Lagrange multiplier method. This method proceeds by first multiplying the original direct problem given by equations (2.23), (2.2) and (2.6) by the Lagrange multiplier $v(x, t)$ and then integrating over the domain. Then, the resulting expression is added to the objective functional J_0 defined by (2.22) to yield

$$J_0(f) = \frac{1}{2} \sum_{k=1}^N \|\ell_k u - h_k\|_{L^2(0, T)}^2 + \int_{Q_T} v(x, t) [\nabla \cdot (A \nabla u) - b(x, t)u + f(x, t)h(x, t) + g(x, t) - u_{tt}] dx dt. \quad (3.4)$$

Given the variation of the above objective functional is $\Delta J_0(f) = J_0(f + \Delta f) - J_0(f)$, and by neglecting second order terms, $J_0(f + \Delta f)$ can be evaluated as follows:

$$J_0(f + \Delta f) = \frac{1}{2} \sum_{k=1}^N \|\ell_k(u + \Delta u) - h_k\|_{L^2(0, T)}^2 + \int_{Q_T} v(x, t) [\nabla \cdot (A \nabla (u + \Delta u)) - b(x, t)(u + \Delta u) + (f(x, t) + \Delta f(x, t))h(x, t) + g(x, t) - (u + \Delta u)_{tt}] dx dt. \quad (3.5)$$

Subtracting $J_0(f)$ given by (3.4) from $J_0(f + \Delta f)$ given above, we obtain

$$\begin{aligned} \Delta J_0(f) &= \frac{1}{2} \sum_{k=1}^N \|\ell_k(u + \Delta u) - h_k\|_{L^2(0,T)}^2 - \frac{1}{2} \sum_{k=1}^N \|\ell_k u - h_k\|_{L^2(0,T)}^2 \\ &\quad + \int_{Q_T} v(x,t) [\nabla \cdot (A \nabla(\Delta u)) - b(x,t)\Delta u + \Delta f(x,t)h(x,t) - (\Delta u)_{tt}] dxdt, \end{aligned} \quad (3.6)$$

$$\begin{aligned} &= \frac{1}{2} \sum_{k=1}^N \|\ell_k \Delta u\|_{L^2(0,T)}^2 + \sum_{k=1}^N \langle \ell_k \Delta u, \ell_k u - h_k \rangle_{L^2(0,T)} \\ &\quad + \int_{Q_T} v(x,t) [\nabla \cdot (A \nabla(\Delta u)) - b(x,t)\Delta u + \Delta f(x,t)h(x,t) - (\Delta u)_{tt}] dxdt. \end{aligned} \quad (3.7)$$

By integrating by parts the terms involving both Δu and v in the right-hand side of the equation above and using the initial and boundary conditions of the sensitivity problem (3.1)-(3.3), we obtain the adjoint problem given by

$$v_{tt} - \nabla \cdot (A \nabla v) + b(x,t)v = \sum_{k=1}^N \omega_k(x)(\ell_k u - h_k), \quad (x,t) \in Q_T, \quad (3.8)$$

$$v(x,T) = v_t(x,T) = 0, \quad x \in \Omega, \quad (3.9)$$

$$v(x,t) = 0, \quad (x,t) \in S_T. \quad (3.10)$$

As $\omega_k \in L^\infty(\Omega) \subset L^2(\Omega)$ and $h_k \in L^2(0,T)$, then $\ell_k u - h_k \in L^2(0,T)$, and it follows that the right-hand side of equation (3.8) is in $L^2(Q_T)$. Then, it can be easily seen that the problem (3.8)-(3.10) is well-posed and it has a unique weak solution in $W(0,T)$.

3.3 The gradient of the objective functional $J_\lambda(f)$

The remaining terms in equation (3.7) are as follows:

$$\Delta J_0(f) = \frac{1}{2} \sum_{k=1}^N \|\ell_k \Delta u\|_{L^2(0,T)}^2 + \int_{Q_T} h(x,t)v(x,t)\Delta f(x,t) dxdt. \quad (3.11)$$

Due to the *a priori* estimate (2.13) for the direct problem (2.23), (2.2) and (2.6), for each $k = \overline{1, N}$, we have

$$\|\ell_k \Delta u\|_{L^2(0,T)}^2 = o(\|\Delta f\|_{L^2(Q_T)}), \quad \text{as } \|\Delta f\|_{L^2(Q_T)} \rightarrow 0. \quad (3.12)$$

The proof of (3.12) is as follows. Since Δu is the solution to the problem (3.1)-(3.3), from the estimate (2.13), we have

$$\max_{t \in [0,T]} \|\Delta u(\cdot, t)\|_{L^2(\Omega)} \leq C \|\Delta f\|_{L^2(Q_T)}.$$

It follows that

$$\begin{aligned} \|\ell_k \Delta u\|_{L^2(0,T)}^2 &= \int_0^T \left| \int_\Omega \omega_k(x) \Delta u(x,t) dx \right|^2 dt \leq \|\omega_k\|_{L^\infty(\Omega)}^2 \int_0^T \int_\Omega \left| \Delta u(x,t) \right|^2 dxdt \\ &\leq C^2 \|\omega_k\|_{L^\infty(\Omega)}^2 \|\Delta f\|_{L^2(Q_T)}^2 = o(\|\Delta f\|_{L^2(Q_T)}). \end{aligned}$$

Then, from (3.11) and (3.12), the following holds

$$\Delta J_0(f) = \int_{Q_T} h(x, t)v(x, t)\Delta f(x, t)dxdt + o(\|\Delta f\|_{L^2(Q_T)}). \quad (3.13)$$

From the right-hand side of equation (3.13) and the definition of the Fréchet derivative, we see that the objective functional J_0 is Fréchet differentiable and its gradient at f is given by

$$\nabla J_0(f) = h(x, t)v(x, t). \quad (3.14)$$

From this equation we can see that for identifiability we need to have that $|h(x, t)| \neq 0$ a.e. in Q_T . Finally, we obtain that the objective functional J_λ given by (2.22) is Fréchet differentiable and its gradient at f is given by

$$\nabla J_\lambda(f) = h(x, t)v(x, t) + \lambda(f(x, t) - f^*(x, t)). \quad (3.15)$$

Remark. If instead of (2.21), the force $F(x, t)$ is sought in the simplified form (2.15), i.e. space-dependent, or (2.16), i.e. time-dependent, then the gradient (3.14) takes the form

$$\nabla J_0(f) = \int_0^T h(x, t)v(x, t)dt, \quad (3.16)$$

or

$$\nabla J_0(f) = \int_\Omega h(x, t)v(x, t)dx, \quad (3.17)$$

respectively. Also, the norm of the regularization term in (2.22) becomes the $L^2(\Omega)$ -norm or the $L^2(0, T)$ -norm, respectively.

In the next subsection, the CGM is described for the minimization of the Tikhonov regularization functional given by (2.22).

3.4 Iterative procedure

In this subsection, the CGM is described for minimizing the objective functional given by (2.22). The following recursive relation is utilized to recover the unknown force $f(x, t)$ in the hyperbolic equation (2.23) starting from an initial guess $f^0(x, t)$:

$$f^{n+1}(x, t) = f^n(x, t) - \gamma_n P_n(x, t), \quad n = 0, 1, \dots, \quad (3.18)$$

where the superscript n denotes the iteration number, γ_n is the search step size used for obtaining the updated version of the missing force $f^{n+1}(x, t)$ from the previously obtained force $f^n(x, t)$, and $P_n(x, t)$ is the direction of descent given by

$$P_n(x, t) = \begin{cases} -\nabla J_\lambda(f^n), & \text{if } n = 0, \\ -\nabla J_\lambda(f^n) + \alpha_n P_{n-1}, & \text{if } n = 1, 2, \dots. \end{cases} \quad (3.19)$$

In equation (3.19), the conjugate coefficient α_n can be found by the Fletcher-Reeves expression given by

$$\alpha_0 = 0, \quad \alpha_n = \frac{\|\nabla J_\lambda(f^n)\|_{L^2(Q_T)}^2}{\|\nabla J_\lambda(f^{n-1})\|_{L^2(Q_T)}^2}, \quad n = 1, 2, \dots. \quad (3.20)$$

The search step size γ_n is computed as the minimizer

$$\gamma_n = \underset{\gamma \geq 0}{\operatorname{argmin}} J_\lambda(f^n - \gamma P_n), \quad n = 0, 1, \dots \quad (3.21)$$

To solve the line search problem given by (3.21), let us first write the solution $u(\cdot, \cdot, f) =: u(f)$ of the problem (2.23), (2.2) and (2.6) as a superposition of the solution denoted by $u(u_0, v_0, g)$ of the problem

$$\begin{cases} u_{tt} - \nabla \cdot (A \nabla u) + b(x, t)u = g(x, t), & (x, t) \in Q_T, \\ u(x, 0) = u_0(x), \quad u_t(x, 0) = v_0(x), & x \in \Omega, \\ u(x, t) = 0, & (x, t) \in S_T, \end{cases} \quad (3.22)$$

and the solution denoted by $u[f]$ of the problem

$$\begin{cases} u_{tt} - \nabla \cdot (A \nabla u) + b(x, t)u = f(x, t)h(x, t), & (x, t) \in Q_T, \\ u(x, 0) = 0, \quad u_t(x, 0) = 0, & x \in \Omega, \\ u(x, t) = 0, & (x, t) \in S_T. \end{cases} \quad (3.23)$$

Then, the observation operator in (2.17) can be recast in the form

$$\ell_k u(f) = \ell_k u[f] + \ell_k u(u_0, v_0, g) = A_k f + \ell_k u(u_0, v_0, g), \quad k = \overline{1, N}, \quad (3.24)$$

where $A_k f := \ell_k u[f]$ is the linear bounded operator from $L^2(Q_T)$ to $L^2(0, T)$ defined from the solution $u[f]$ to the problem (3.23) via the integral relation (2.17). Remark that from the similarity between the problem (3.23) and the sensitivity problem (3.1)-(3.3) we have that $\ell_k \Delta u = A_k f$.

To evaluate the search step size γ_n we set $\Delta f^n(x, t) = P_n(x, t)$ and linearize $u(x, t; f^n - \gamma P_n)$ by a first-order Taylor series expression to obtain

$$u(x, t; f^n - \gamma P_n) \approx u(x, t; f^n) - \gamma P_n \frac{\partial u}{\partial f^n}(x, t; f^n) \approx u(x, t; f^n) - \gamma \Delta u(x, t; f^n), \quad (3.25)$$

where $\Delta u(x, t; f^n)$ is obtained by solving the sensitivity problem (3.1)-(3.3) with $\Delta f^n(x, t) = P_n(x, t)$. Then, differentiating $J_\lambda(f^n - \gamma P_n)$ with respect to γ and making it zero, we obtain

$$\gamma_n = \frac{\sum_{k=1}^N \langle \ell_k \Delta u(f^n), \ell_k u(f^n) - h_k \rangle_{L^2(0, T)} + \lambda \langle P_n, f^n - f^* \rangle_{L^2(Q_T)}}{\sum_{k=1}^N \|\ell_k \Delta u(f^n)\|_{L^2(0, T)}^2 + \lambda \|P_n\|_{L^2(Q_T)}^2}. \quad (3.26)$$

In equation (3.26), remark that $\ell_k u(f^n) - h_k$ can be calculated from

$$\ell_k u(f^n) - h_k = \ell_k \Delta u(f^n) + \ell_k u(u_0, v_0, g) - h_k = \ell_k \Delta u(f^n) + \hat{h}_k, \quad (3.27)$$

where $\hat{h}_k := \ell_k u(u_0, v_0, g) - h_k$ does not depend on the iteration number n , and can be calculated independently by solving the direct problem (3.22).

3.5 Algorithm

The CGM proceeds as described in the following steps:

1. Set $n = 0$ and select an initial guess $f^0 \in L^2(Q_T)$ equal to an *a priori* given estimate $f^* \in L^2(Q_T)$.
2. Solve the direct problem given by equations (2.23), (2.2) and (2.6) to obtain $u(x, t; f^n)$ and compute $J_\lambda(f^n)$ from equation (2.22).
3. Solve the adjoint problem given by equations (3.8)-(3.10) to find $v(x, t; f^n)$. Compute the gradient $\nabla J_\lambda(f^n)$ from equation (3.15), the conjugate coefficient α_n from equation (3.20), and the direction of descent $P_n(x, t)$ from equation (3.19).
4. Solve the sensitivity problem given by equations (3.1)-(3.3) to obtain $\Delta u(x, t; f^n)$ by taking $\Delta f^n(x, t) = P_n(x, t)$ and compute the search step size γ_n from equation (3.26).
5. Update $f^{n+1}(x, t)$ from equation (3.18).
6. Stop if the desired level of accuracy has been achieved, else set $n = n + 1$ and go to step 2.

4 Numerical results and discussion

We use the finite-difference method (FDM), as in Dai and Nassar (1999), based on the Crank-Nicolson scheme in one dimension $d = 1$ with mesh size Δx and time step Δt , or the alternating direction implicit (ADI) scheme, as in Araújo et al. (2014), relying on the Peaceman-Rachford splitting strategy in two dimensions $d = 2$ with mesh sizes Δx_1 and Δx_2 , and time step Δt , to solve the direct, sensitivity and adjoint problems in the CGM described in Section 3.5. Alternatively, the finite element method could be used, see e.g. Johanson (1993). The trapezoidal rule is used for discretizing the integrals in equations (3.20) and (3.26). The error functional, as a function of the number of iterations n , is defined as

$$E(f^n) = \|f^n - f\|_{L^2(Q_T)}, \quad (4.1)$$

where f^n stands for the numerical result obtained by the CGM at the iteration number n and f denotes the true force function, if available.

In the inversion below we consider both noise-free and noisy data. While the noise-free data h_k for $k = \overline{1, N}$ are obtained from the available analytical solution $u(x, t)$, the noisy data $h_k^{(\epsilon_k)}$ for $k = \overline{1, N}$, satisfying

$$\|h_k^{(\epsilon_k)} - h_k\|_{L^2(0, T)} \leq \epsilon_k, \quad k = \overline{1, N}, \quad (4.2)$$

where $\epsilon_k \geq 0$ is the amount of noise, is numerically simulated as

$$h_k^{(\epsilon_k)}(t_l) = h_k(t_l) + \epsilon_l^{(k)}, \quad l = \overline{1, M}, \quad (4.3)$$

where $t_l = lT/M$ for $l = \overline{1, M}$ and, for each $k = \overline{1, N}$, $(\epsilon_l^{(k)})_{l=\overline{1, M}}$ are M random variables generated from a Gaussian normal distribution with zero mean and standard deviation given by

$$\sigma_k = p \times \max_{t \in [0, T]} |h_k(t)|, \quad k = \overline{1, N}, \quad (4.4)$$

where p represents the percentage of noise. In MATLAB, this is realized using the command *normrnd* to generate the random variables $\epsilon^{(k)} = (\epsilon_l^{(k)})_{l=\overline{1, M}}$ as follows:

$$\epsilon^{(k)} = \text{normrnd}(0, \sigma_k, M), \quad k = \overline{1, N}. \quad (4.5)$$

The total amount of noise ϵ is given by

$$\epsilon = \sqrt{\sum_{k=1}^N \|h_k^{(\epsilon_k)} - h_k\|_{L^2(0, T)}^2}. \quad (4.6)$$

The convergence, accuracy and stability of the proposed CGM for inversion is verified in one and two dimensions in the next two subsections.

4.1 Example 1 (one-dimensional example)

Taking $d = 1$, $\Omega = (0, 1)$, $T = 1$, and the input data

$$a_{11}(x, t) = 1, \quad b(x, t) = 1, \quad h(x, t) = 1, \quad (4.7)$$

$$u(x, 0) = u_0(x) = x - x^2, \quad \frac{\partial u}{\partial t}(x, 0) = v_0(x) = x - x^2, \quad (4.8)$$

$$g(x, t) = 2[(x - x^2)e^t + e^t] - (1 - t) \sin(\pi x), \quad (4.9)$$

and considering the force

$$f(x, t) = (1 - t) \sin(\pi x), \quad (4.10)$$

it can be verified by direct substitution that the analytical solution of the direct problem given by equations (2.23), (2.2) and (2.6) is given by

$$u(x, t) = (x - x^2)e^t. \quad (4.11)$$

To investigate the influence of the number of observations N on the accuracy of reconstructing the force $f(x, t)$ for the inverse problem given by equations (2.23), (2.2), (2.6) and (2.17) with unknown force $f(x, t)$ and displacement $u(x, t)$ we take $N = 1$ ($\xi^1 = 0.5$), $N = 3$ ($\xi^1 = 0.3$, $\xi^2 = 0.5$ and $\xi^3 = 0.7$), and $N = 5$ ($\xi^1 = 0.1$, $\xi^2 = 0.3$, $\xi^3 = 0.5$, $\xi^4 = 0.7$ and $\xi^5 = 0.9$) observation points, and use the average weighted integral observations (2.20) with $\Omega_k = (\xi^k - \Delta x, \xi^k + \Delta x)$ of length $|\Omega_k| = 2\Delta x$ for $k = \overline{1, 5}$. This yields

$$h_k(t) = -\frac{1}{3}e^t [(\Delta x)^2 + 3(\xi^k - 1)\xi^k], \quad t \in (0, 1), \quad k = \overline{1, 5}. \quad (4.12)$$

In practice, f^* is usually taken as the mean average of f , namely, $f^* = \frac{1}{|Q_T|} \int_{Q_T} f(x, t) dx dt$, see Thanh (2020); however, in this section we take it arbitrary, say $f^* = 0$. Then, with the

initial guess $f^0 = 0$ we run the CGM described in Section 3.5 with $\Delta t = \Delta x = 0.025$, $p = 0$, i.e. no noise, and $\lambda = 10^{-5}$ for 20 iterations. Figure 1(a) and (b) show the true (4.10) and numerical forces at $(0.5, t)$, as functions of $t \in [0, 1]$, and at $(x, 0.5)$, as functions of $x \in [0, 1]$, respectively, for $N \in \{1, 3, 5\}$. From these figures, it can be seen that increasing the number of observations N renders the reconstructed force $f(x, t)$ more accurate.

Next, we fix $N = 5$ and run the CGM described in Section 3.5 with $\Delta t = \Delta x = 0.025$ and $p \in \{0, 1\}\%$ noise for 20 iterations. We take $\lambda = 10^{-5}$ for $p = 0$, i.e. no noise, while for $p = 1\%$ we take $\lambda = 2.1 \times 10^{-3}$ as dictated by the discrepancy principle illustrated in Figure 2 to obtain a stable solution. Figures 3(a) and (b) show the monotonic decreasing convergence of the objective functional $J_\lambda(f^n)$ defined by (2.22) and the error functional $E(f^n)$ defined by (4.1), respectively, as functions of the number of iterations n . Figure 4 presents the numerical reconstructions of the force $f(x, t)$ in comparison with the true force (4.10). To elaborate more on the convergence, Figures 5(a) and (b) depict the true (4.10) and numerical forces at $(0.5, t)$, as functions of $t \in [0, 1]$, and at $(x, 0.5)$, as functions of $x \in [0, 1]$, respectively, for exact and noisy data. From Figures 4 and 5, it can be seen that stable and reasonably accurate solutions have been achieved.

4.2 Example 2 (two-dimensional example)

In this two-dimensional example, we take $d = 2$, $\Omega = (0, 1) \times (0, 1)$, $T = 1$, and the input data

$$a_{ij}(x_1, x_2, t) = \delta_{ij}, \quad i, j = 1, 2, \quad b(x_1, x_2, t) = 1, \quad h(x_1, x_2, t) = 1, \quad (4.13)$$

$$u(x_1, x_2, 0) = u_0(x_1, x_2) = (x_1 - x_1^2) \sin(\pi x_2), \quad (4.14)$$

$$\frac{\partial u}{\partial t}(x_1, x_2, 0) = v_0(x_1, x_2) = (x_1 - x_1^2) \sin(\pi x_2), \quad (4.15)$$

$$g(x_1, x_2, t) = \left\{ [(\pi^2 + 2)e^t - \sin(\pi t)](x_1 - x_1^2) + 2e^t \right\} \sin(\pi x_2), \quad (4.16)$$

and consider the force

$$f(x_1, x_2, t) = (x_1 - x_1^2) \sin(\pi x_2) \sin(\pi t). \quad (4.17)$$

It can be verified by direct substitution that the analytical solution of the direct problem given by equations (2.23), (2.2) and (2.6) is given by

$$u(x_1, x_2, t) = (x_1 - x_1^2) \sin(\pi x_2) e^t. \quad (4.18)$$

For the inverse problem given by equations (2.23), (2.2), (2.6) and (2.17) with unknown force $f(x_1, x_2, t)$ and displacement $u(x_1, x_2, t)$ we take $N = 9$ observation points $\xi^k = (\xi_1^k, \xi_2^k)$ for $k = \overline{1, 9}$, as $\xi^1 = (0.1, 0.4)$, $\xi^2 = (0.2, 0.7)$, $\xi^3 = (0.4, 0.1)$, $\xi^4 = (0.5, 0.6)$, $\xi^5 = (0.5, 0.9)$, $\xi^6 = (0.6, 0.4)$, $\xi^7 = (0.7, 0.2)$, $\xi^8 = (0.8, 0.8)$ and $\xi^9 = (0.9, 0.5)$, and use the average weighted integral observations (2.20) with $\Omega_k = (\xi_1^k - \Delta x_1, \xi_1^k + \Delta x_1) \times (\xi_2^k - \Delta x_2, \xi_2^k + \Delta x_2)$ of area $|\Omega_k| = 4\Delta x_1 \Delta x_2$ for $k = \overline{1, 9}$. This yields

$$h_k(t) = \frac{e^t}{\pi \Delta x_2} \left\{ \xi_1^k - (\xi_1^k)^2 - \frac{(\Delta x_1)^2}{3} \right\} \sin(\pi \xi_2^k) \sin(\pi \Delta x_2), \quad t \in (0, 1), \quad k = \overline{1, 9}. \quad (4.19)$$

We also take the *a priori* estimate $f^* = 0$ and the initial guess $f^0 = 0$, and run the CGM described in Section 3.5 with the ADI-FDM mesh sizes $\Delta t = \Delta x_1 = \Delta x_2 = 0.025$ and $p \in \{0, 1\}\%$ noise for 20 iterations. We take $\lambda = 10^{-3}$ for $p = 0$, i.e. no noise, while for $p = 1\%$ we take $\lambda = 1.5 \times 10^{-2}$ as dictated by the discrepancy principle illustrated in Figure 6 to restore the stability of the solution.

Figures 7(a) and (b) show the monotonic decreasing convergence of the objective functional $J_\lambda(f^n)$ defined by (2.22) and the error functional $E(f^n)$ defined by (4.1), respectively, as functions of the number of iterations n . Figure 8 shows the reconstructions of the force $f(x_1, x_2, t)$ at $(x_1, x_2, 0.5)$ in comparison with the analytical force (4.17), as functions of $(x_1, x_2) \in [0, 1] \times [0, 1]$. In addition, Figure 9 depicts the analytical (4.17) and recovered forces at $(0.4, 0.5, t)$, as functions of $t \in [0, 1]$, for exact and noisy data. From Figures 8 and 9, it can be seen that stable and reasonably accurate solutions have been accomplished.

5 Conclusions

In this paper, a new formulation to determine general space- and time-dependent forces from many average integral observations in hyperbolic PDE's has been attempted. This linear but ill-posed inverse problem formulated as a minimization problem still encounters non-uniqueness issues, but we can at least reconstruct that force solution which is the closest to an *a priori* given estimate f^* . Stability of reconstruction has been ensured using the Tikhonov regularization method. The Tikhonov regularization functional has been proved to be Fréchet differentiable and a formula for its Fréchet gradient has been derived. The CGM has been applied for minimizing iteratively the Tikhonov regularization functional with the discrepancy principle employed for selecting the regularization parameter. The finite-difference numerically obtained results illustrate the accuracy and stability of the numerical reconstruction.

The approach described in this paper can easily be extended to fourth-order evolution PDE's, e.g. identifying the load in the Euler-Bernoulli beam equation, but this extension will be undertaken in a future work.

Acknowledgements

M. Alosaimi would like to thank Taif University in Saudi Arabia and the United Kingdom Saudi Arabian Cultural Bureau (UKSACB) in London for supporting his PhD studies at the University of Leeds. D. Lesnic would like to acknowledge some small financial support received from the EPSRC funded research network on Inverse Problems EP/P005985/1 for a couple of days research visit of Professor Dinh Nho Hào to Leeds in July 2019.

References

- [1] N.L. Abasheeva (2009) *Identification of a source for parabolic and hyperbolic equations with a parameter*, J. Inverse Ill-Posed Probl., **17**, 527–544.
- [2] A.Kh. Amirov (1987) *On the question of solvability of inverse problems*, Dokl. Math., **34**, 258–259.
- [3] A. Araújo, C. Neves and E. Sousa (2014) *An alternating direction implicit method for a second-order hyperbolic diffusion equation with convection*, Appl. Math. Comput., **239**, 17–28.
- [4] J.R. Cannon and D.R. Dunninger (1970) *Determination of an unknown forcing function in a hyperbolic equation from overspecified data*, Ann. Mat. Pura Appl., **85**, 49–62.
- [5] M.D. Collins and W.A. Kuperman (1994) *Inverse problems in ocean acoustics*, Inverse Probl., **10**, 1023–1040.
- [6] D. Colton and R. Kress (2013) *Inverse Acoustic and Electromagnetic Scattering Theory*, 3rd edn., Springer-Verlag, New York.
- [7] W. Dai and R. Nassar (1999) *A finite difference scheme for solving the heat transport equation at the microscale*, Numer. Meth. Part Differ. Equ., **15**, 697–708.
- [8] A. El Badia and T. Ha-Duong (2001) *Determination of point wave sources by boundary measurements*, Inverse Probl., **17**, 1127–1139.
- [9] H.W. Engl, O. Scherzer and M. Yamamoto (1994) *Uniqueness and stable determination of forcing terms in linear partial differential equations with overspecified boundary data*, Inverse Probl., **10**, 1253–1276.
- [10] L.C. Evans (1998) *Partial Differential Equations*, American Mathematical Society, Providence, R.I..
- [11] D.N. Hào, B.V. Huong, N.T. Oanh and P.X. Thanh (2017) *Determination of a term in the right-hand side of parabolic equations*, J. Comput. Appl. Math., **309**, 28–43.
- [12] A. Hasanov (2009) *Simultaneous determination of the source terms in a linear hyperbolic problem from the final overdetermination: weak solution approach*, IMA J. Appl. Math., **74**, 1–19.
- [13] C.-H. Huang (2001) *An inverse non-linear force vibration problem of estimating the external forces in a damped system with time-dependent system parameters*, J. Sound Vibr., **242**, 749–765.
- [14] S.O. Hussein and D. Lesnic (2014) *Determination of a space-dependent source function in the one-dimensional wave equation*, Electron. J. Bound. Elem., **12**, 1–26.
- [15] S.O. Hussein and D. Lesnic (2016a) *Determination of forcing functions in the wave equation. Part I: The space-dependent case*, J. Eng. Math., **96**, 115–133.

- [16] S.O. Hussein and D. Lesnic (2016b) *Determination of forcing functions in the wave equation. Part II: The time-dependent case*, J. Eng. Math., **96**, 135–153.
- [17] S.O. Hussein (2016) *Inverse Force Problems for the Wave Equation*, PhD Thesis, University of Leeds, UK.
- [18] V. Isakov (1998) *Inverse Problems for Partial Differential Equations*, Springer, Berlin.
- [19] C. Johanson (1993) *Discontinuous Galerkin finite element methods for second order hyperbolic problems*, Comput. Meth. Appl. Mech. Eng., **107**, 117–129.
- [20] M.V. Klibanov (1992) *Inverse problems and Carleman estimates*, Inverse Probl., **8**, 575–596.
- [21] N.I. Kozhanov and R.R. Safiullova (2010) *Linear inverse problems for parabolic and hyperbolic equations*, J. Inverse Ill-Posed Probl., **18**, 1–24.
- [22] O.A. Ladyzhenskaya (1985) *The Boundary Value Problems of Mathematical Physics*, Springer-Verlag, New York.
- [23] D. Lesnic, S.O. Hussein and B.T. Johansson (2016) *Inverse space-dependent force problems for the wave equation*, J. Comput. Appl. Math., **306**, 10–39.
- [24] Ş. Özen, S. Helhel and O. Çerezci (2008) *Heat analysis of biological tissue exposed to microwave by using thermal wave model of bio-heat transfer (TWMBT)*, Burns, **34**, 45–49.
- [25] A.I. Prilepko, D.G. Orlovsky and I.A. Vasin (2000) *Methods for Solving Inverse Problems in Mathematical Physics*, Marcel Dekker, Inc., New York.
- [26] K. Rashedi and M. Sini (2015) *Stable recovery of the time-dependent source term from one measurement for the wave equation*, Inverse Probl., **31**, 105011, (17 pages).
- [27] B. Sjögreen and N.A. Petersson (2014) *Source estimation by full wave from inversion*, J. Sci. Comput., **59**, 247–276.
- [28] P.X. Thanh (2020) *Space-time finite element method for determination of a source in parabolic equations from boundary observations*, J. Inverse Ill-Posed Probl., (accepted).
- [29] P.N. Vabishchevich (2019) *Computational identification of the time dependence of the right-hand side of a hyperbolic equation*, Comput. Math. Math. Phys., **59**, 1475–1483.
- [30] M. Yamamoto (1995) *Stability, reconstruction formula and regularization for an inverse source hyperbolic problem by a control method*, Inverse Probl., **11**, 481–496.

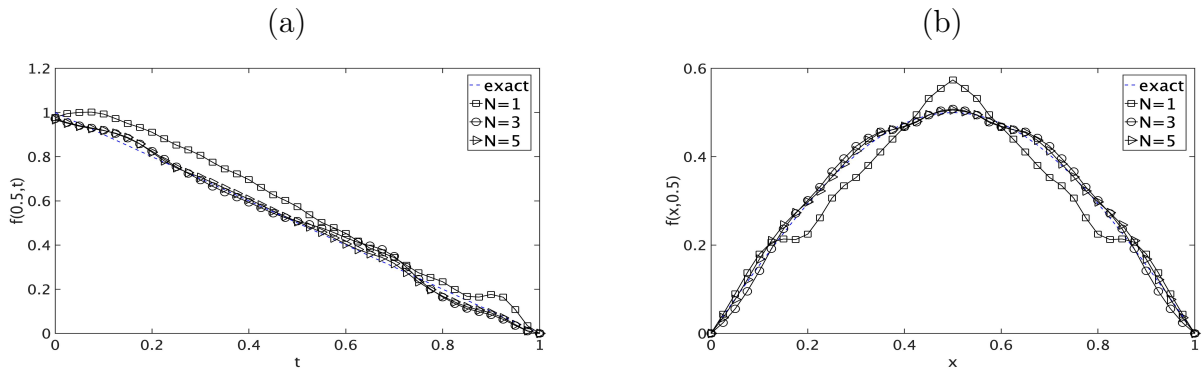


Figure 1: The analytical (4.10) and numerical forces $f(x, t)$ at (a) $(0.5, t)$, as functions of $t \in [0, 1]$, and at (b) $(x, 0.5)$, as functions of $x \in [0, 1]$, for $N \in \{1, 3, 5\}$ with $p = 0$, i.e. no noise, for Example 1.

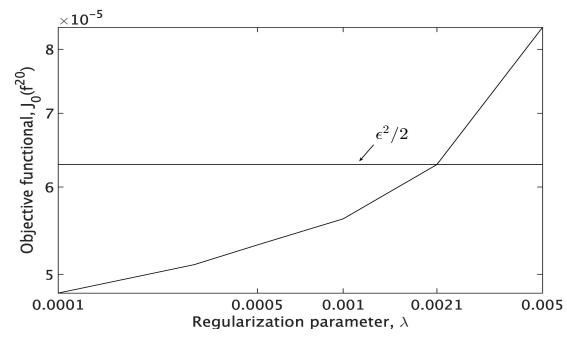


Figure 2: The objective functional $J_0(f^{20})$ after 20 iterations, as a function of λ , for $p = 1\%$ noise, for Example 1.

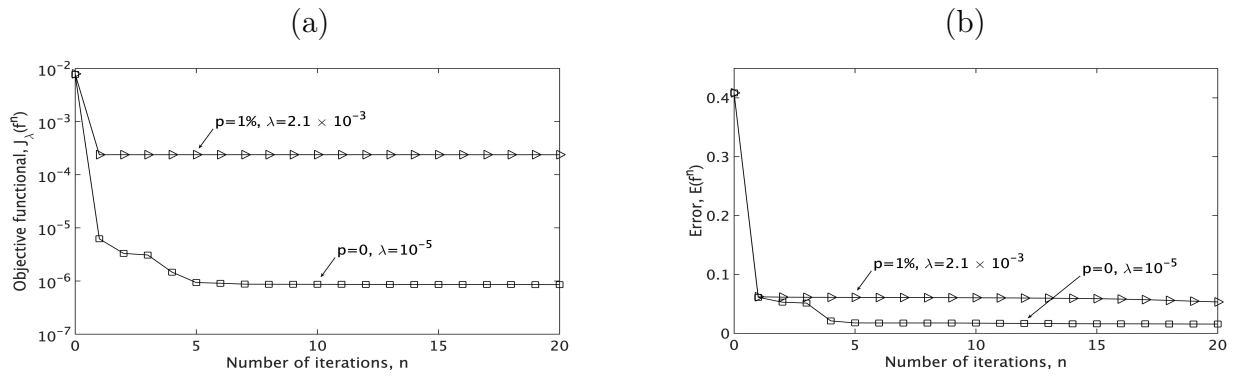


Figure 3: (a) The objective functional $J_\lambda(f^n)$ and (b) the error functional (4.1), with $p \in \{0, 1\}\%$ noise, for Example 1.

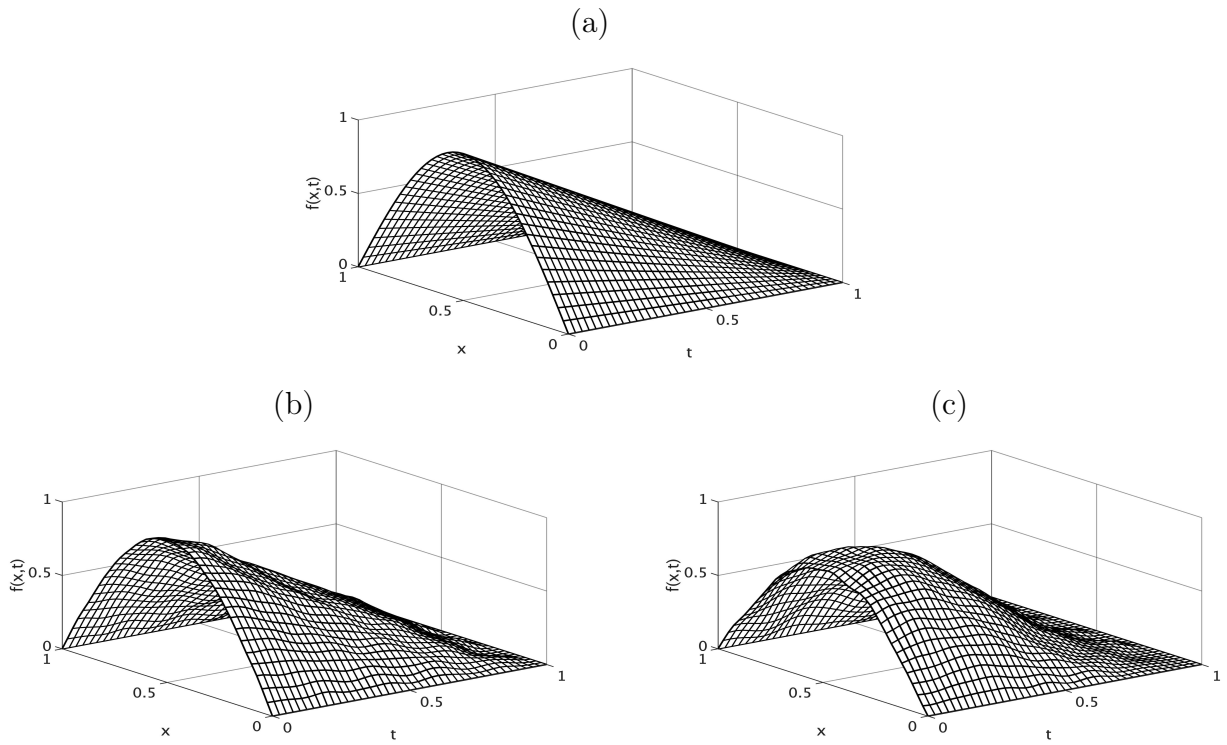


Figure 4: (a) The analytical (4.10) and numerical forces $f(x, t)$ with (b) $p = 0$ and $\lambda = 10^{-5}$, and (c) $p = 1\%$ noise and $\lambda = 2.1 \times 10^{-3}$, for Example 1.

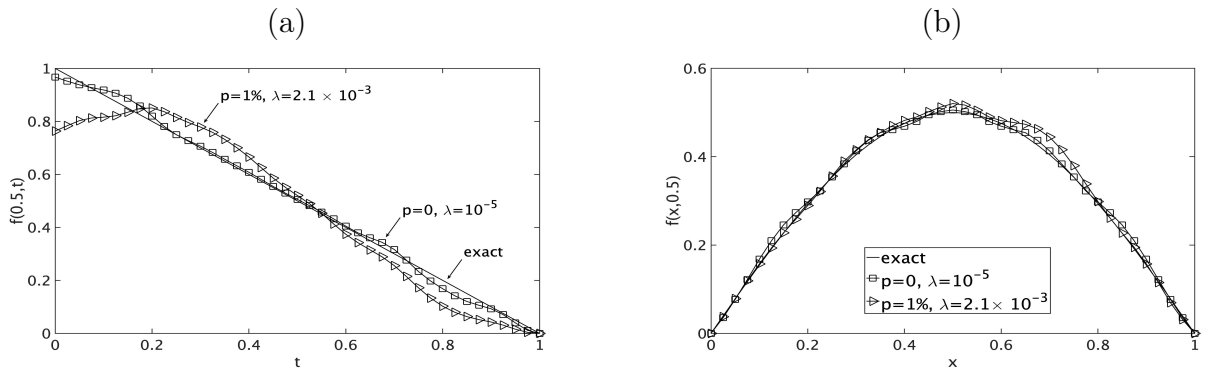


Figure 5: The analytical (4.10) and numerical forces $f(x, t)$ at (a) $(0.5, t)$, as functions of $t \in [0, 1]$, and at (b) $(x, 0.5)$, as functions of $x \in [0, 1]$, with $p \in \{0, 1\}\%$ noise, for Example 1.

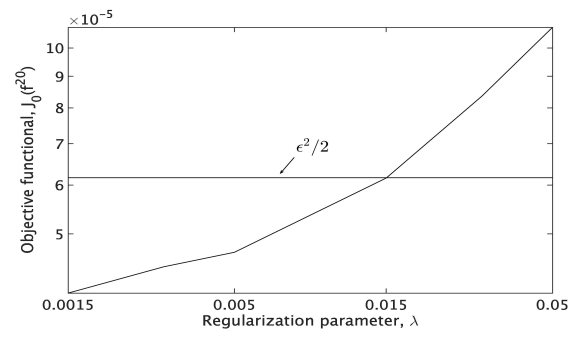


Figure 6: The objective functional $J_0(f^{20})$ after 20 iterations, as a function of λ , for $p = 1\%$ noise, for Example 2.

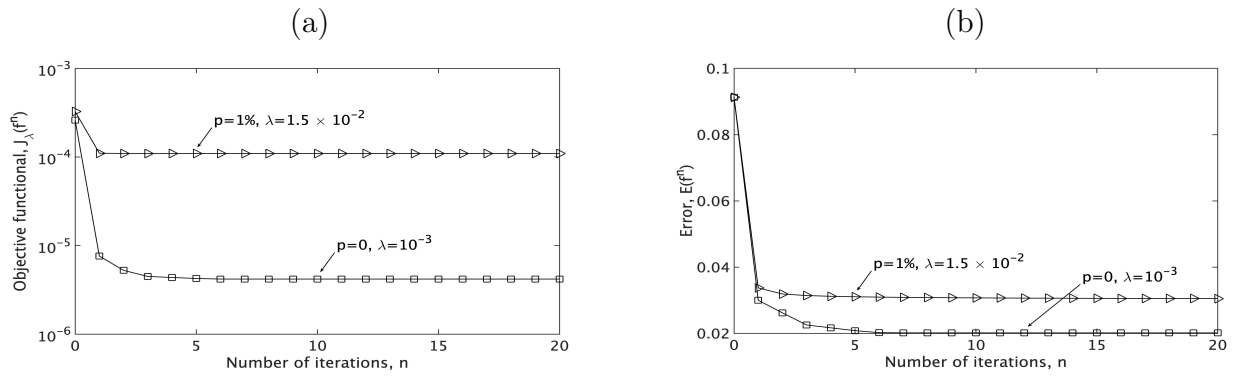


Figure 7: (a) The objective functional $J_\lambda(f^n)$ and (b) the error functional (4.1), with $p \in \{0, 1\}\%$ noise, for Example 2.

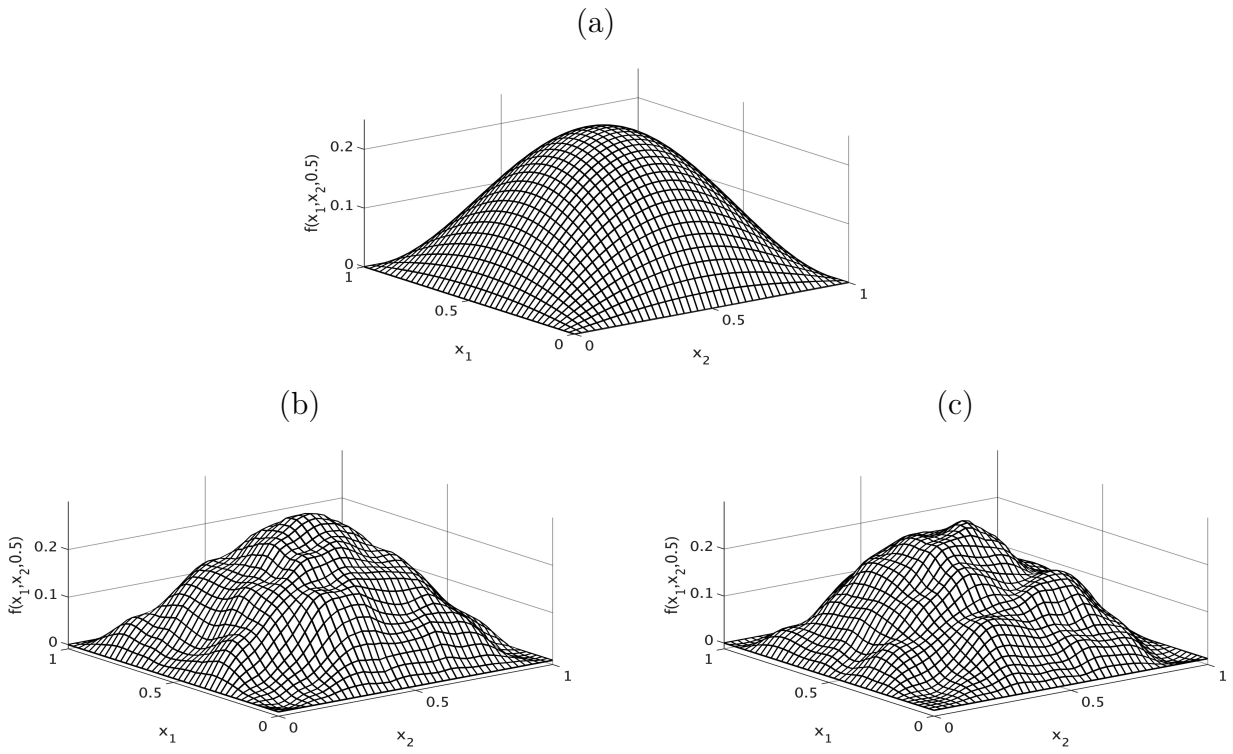


Figure 8: (a) The analytical (4.17) and numerical forces $f(x_1, x_2, t)$ at $(x_1, x_2, 0.5)$ with (b) $p = 0$ and $\lambda = 10^{-3}$, and (c) $p = 1\%$ noise and $\lambda = 1.5 \times 10^{-2}$, for Example 2.

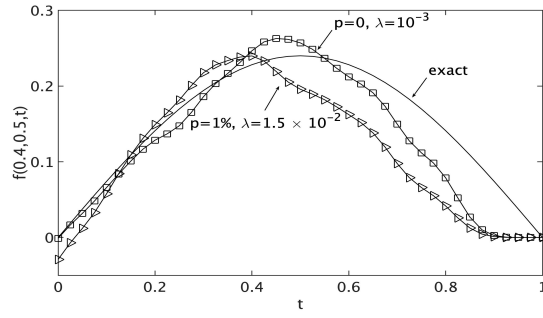


Figure 9: The analytical (4.17) and numerical forces $f(x_1, x_2, t)$ at $(0.4, 0.5, t)$, as functions of $t \in [0, 1]$, with $p \in \{0, 1\}\%$ noise, for Example 2.